



ROBUST RADIAL DISTORTION CORRECTION BASED ON ALTERNATE OPTIMIZATION

Juan Andrade and Lina J. Karam

School of Electrical, Computer and Energy Engineering
 Arizona State University, Tempe, AZ, 85282-5706, USA
 email:(jmandrad,lkaram)@asu.edu

ABSTRACT

A robust radial distortion correction method that requires only a single image of the distorted imaged pattern is presented. The method is robust to the orientation of the imaged pattern and does not require the availability of the ideal reference regularly structured pattern which can be recreated from detected features in the distorted image. Radial distortion parameters, i.e., the Center of Distortion (CoD) and radial distortion coefficients (RDC), are optimized by minimizing corresponding cost functions in an alternate manner. Tests with synthetic and real data are presented in order to illustrate the performance robustness of the proposed algorithm.

Index Terms— Radial distortion, center of distortion, single image, alternate optimization.

1. INTRODUCTION

The pinhole camera model is frequently used in computer vision applications in order to project 3D scene points to 2D image points; however, off-the-shelf cameras do not precisely satisfy the ideal pinhole model due to lens distortion and mounting defects. Although the overall distortion results from the combination of radial, decentering and thin prism distortion [1], the last two are usually negligible for most of the commercial cameras [2]. Consequently, radial distortion (RD) is frequently the source of distortion that is modeled. Furthermore, it has been shown that more elaborate models not only provide a negligible improvement but they can also cause numerical instability [3]. RD can be a significant factor of distortion in wide angle and low focal length lenses.

This paper presents a novel radial distortion correction (RDC) method that requires only the distorted image of a regularly structured pattern and that does not require availability of the corresponding ideal reference pattern. The proposed RDC method is based on an alternating optimization process where the estimated CoD and radial distortion model parameters are refined through alternate minimization of two corresponding cost functions.

This paper is organized as follows. Section 2 provides a background related to radial distortion correction. In Section 3 the proposed algorithm is described in detail. Quantita-

tive and qualitative results are presented in Section 4. Finally a conclusion is provided in Section 5.

2. BACKGROUND

Based on the pinhole camera model, a three-dimensional scene point is ideally represented on the image plane by the undistorted pixel $P_u = (x_u, y_u)$; however, due to radial distortion, the position of P_u is radially displaced with respect to the Center of Distortion (CoD) along the line that links the CoD and P_u resulting in the distorted pixel $P_d = (x_d, y_d)$.

Many distortion models have been proposed [1, 4, 5, 6, 7, 8]; however, the most used ones are [1] and [6]. In the even-order polynomial model [1], the distorted (x_d, y_d) and undistorted (x_u, y_u) pixels are related as follows:

$$\begin{aligned} x_u &= (x_d - C_x)F(\Lambda) + C_x \\ y_u &= (y_d - C_y)F(\Lambda) + C_y \end{aligned} \quad (1)$$

where (C_x, C_y) denotes the location of the CoD in pixels with respect to the top-left corner of the image, $\Lambda = [\lambda_1, \lambda_2, \dots, \lambda_L]$ is the set of RDC, and $F(\Lambda)$ is given by:

$$F(\Lambda) = 1 + \sum_{i=1}^L \lambda_i r_d^{2i} \quad (2)$$

In (2), r_d is the normalized Euclidean distance between the distorted pixel P_d and the CoD given by:

$$r_d = \sqrt{\left(\frac{x_d - C_x}{\gamma}\right)^2 + \left(\frac{y_d - C_y}{\gamma}\right)^2} \quad (3)$$

where the normalization factor γ is defined as the diagonal length of the input image.

An alternative model [6], known as the division model, which can handle distortions with lower orders than the polynomial model, is given by:

$$\begin{aligned} x_u &= \frac{(x_d - C_x)}{F(\Lambda)} + C_x \\ y_u &= \frac{(y_d - C_y)}{F(\Lambda)} + C_y \end{aligned} \quad (4)$$

Practical tests [9, 10, 3] have shown that the use of more than two parameters ($L > 2$ in Equation (2)) provides no sig-

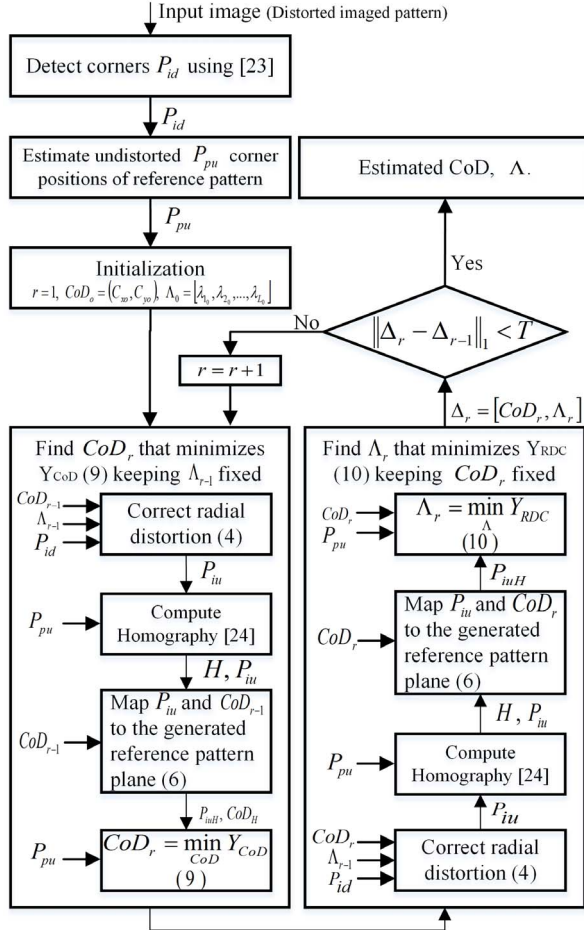


Fig. 1. Flowchart of the proposed algorithm.

nificant improvement; moreover, it was shown that the estimation of less parameters is more robust [10, 11].

Many methods have been proposed for estimating radial distortion parameters. Radial distortion (RD) correction methods can be broadly classified into three groups. The first group consists of methods that make use of known features in a single image of a calibration pattern. The used pattern can be planar [1, 3, 4, 9, 12, 13] or tridimensional [7, 14]. The second group consists of methods that make use of correspondences across multiple images [3, 4, 6, 7, 8, 14, 15, 16, 17, 18]. Multi-view methods use feature correspondences among images and projective geometry [15]. Besides requiring multiple images, these methods require the imaged scene to be static and non-deformable. A multi-camera calibration is presented in [19], it uses a single image of multiple checkerboards placed at different locations in the scene instead of multiple images of a single checkerboard. The third group consists of methods known as plumb-line methods which exploit the fact that tridimensional straight lines in the scene are imaged as curves [2, 4, 8, 10, 20, 21, 22, 23]. These approaches are well suited for images that include man-made structure i.e., images con-

taining straight lines. In most cases, these latter methods require user intervention in order to specify which lines in the image are straight lines in the scene. Since RD correction is a non-linear problem most of the proposed methods have an iterative nature. Closed form solutions can be reached under certain constraints that limit the accuracy or robustness. Some approaches [6, 16] consider the CoD to be known a-priori or assume it to be the image center. However, in [7] it is indicated that the CoD has a considerable offset with respect to the image center.

3. PROPOSED ALGORITHM

The flowchart of the proposed algorithm is shown in Fig. 1. The procedure starts with a single image of the pattern which may include radial distortion, blurring and noise. The algorithm proposed in [19], whose implementation is freely available, was used to define the positions of corners in the distorted image, i.e., $P_{id}^k = (x_{id}^k, y_{id}^k)$, $k = 1, 2, \dots, N$, where N is the total number of detected corner features. Based on the structure of the detected features P_{id} , the undistorted positions of the corners of a regularly structured reference pattern $P_{pu}^k = (x_{pu}^k, y_{pu}^k)$, $k = 1, 2, \dots, N$ are estimated considering a regular rectangular array.

The radial distortion parameters are initialized as follows. The position of the CoD is initialized as the center of the input image. Although we tested other more complex initialization methods for the CoD such as the ones provided by [6], [15] these resulted in no significant improvement neither in accuracy of the radial distortion correction nor in processing time. The radial distortion coefficients Λ were initialized with the value of 0.1.

3.1. Radial distortion correction

Let $P_{id}^k = (x_{id}^k, y_{id}^k)$ be the k^{th} corner detected in the distorted imaged pattern, $k = 1, 2, \dots, N$, where N is the total number of detected features. Radial distortion correction is applied to P_{id}^k according to (4). The resulting undistorted corners' positions $P_{iu}^k = (x_{iu}^k, y_{iu}^k)$, $k = 1, 2, \dots, N$ are used to compute a homography that will be used to map P_{iu}^k to the pattern plane.

3.2. Computation of the Homography

Let (x_1, y_1) and (x_2, y_2) be a pair of corresponding scene features of a planar surface under two different views. In a distortion free situation such pairs are related by a homography [24] as follows:

$$[x_1, y_1, 1]^T = H \cdot [x_2, y_2, 1]^T \quad (5)$$

Since radial distortion is present we need to determine the Homography H that best models the correspondences $P_{iu} \leftrightarrow P_{pu}$ using (5). The computed homography H is used to map undistorted pattern corners P_{iu} as well as the current position

Table 1. Comparison of average radial distortion error between the method presented in [13] and the proposed one. The performance is evaluated for different levels of radial distortion given by $-0.9 \leq \lambda_{1d} \leq -0.1$ and different amounts of noise given by σ added to the ground-truth distorted corners positions in the testing image.

λ_{1d}	Proposed algorithm							Algorithm [13]						
	$\sigma=0$	$\sigma=0.5$	$\sigma=1$	$\sigma=1.5$	$\sigma=2$	$\sigma=2.5$	$\sigma=3$	$\sigma=0$	$\sigma=0.5$	$\sigma=1$	$\sigma=1.5$	$\sigma=2$	$\sigma=2.5$	$\sigma=3$
-0.9	29.19	27.52	27.39	26.58	27.21	27.26	28.21	42.54	41.03	41.60	42.42	43.19	43.97	43.39
-0.8	11.83	10.96	10.88	10.70	10.71	11.41	10.88	19.86	19.32	19.29	19.88	20.66	21.48	23.32
-0.7	4.67	4.30	4.29	4.06	4.05	3.77	4.03	9.36	8.70	8.07	7.78	6.29	5.48	4.71
-0.6	1.81	1.59	1.60	1.57	1.27	1.51	1.86	5.50	4.58	4.80	4.84	4.59	4.52	4.34
-0.5	0.67	0.61	0.38	0.40	0.33	0.68	0.72	3.61	3.38	3.49	3.06	0.36	2.74	7.05
-0.4	0.23	0.20	0.03	0.11	0.23	0.17	0.30	1.42	0.98	0.50	0.55	2.88	5.82	1.29
-0.3	0.07	0.10	0.08	0.09	0.14	0.29	0.09	1.02	0.68	0.15	1.98	3.52	5.23	5.65
-0.2	0.02	0.00	0.03	0.07	0.00	0.11	0.09	0.08	0.33	1.65	2.59	0.40	3.68	3.02
-0.1	0.00	0.01	0.05	0.01	0.06	0.39	0.31	0.53	0.33	1.16	2.00	1.02	1.02	1.81

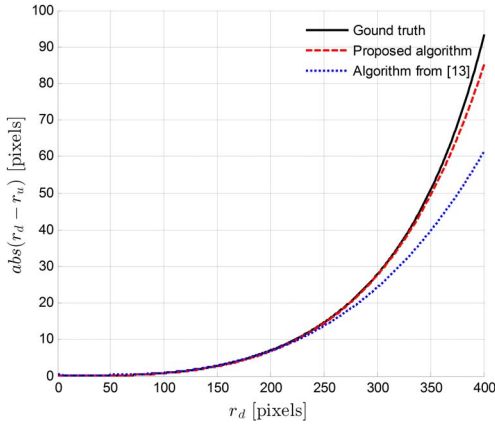


Fig. 2. Graph of radial distortion $|r_d - r_u|$ versus radial distorted positions r_d for a pattern distorted according to (12) with $\lambda_{1d} = -0.5$. Noiseless positions of the pattern corners were used. The image resolution is 640×480 .

of the $CoD = (C_x, C_y)$ from the image plane to the pattern plane as follows:

$$\begin{aligned} P_{iuH}^k &= H \cdot P_{iu}^k \quad \forall k \\ CoD_H &= H \cdot CoD \end{aligned} \quad (6)$$

where the homogeneous notation has been omitted for convenience. These mapped features together with the reconstructed undistorted reference pattern positions P_{pu} are used to compute the appropriated cost functions.

3.3. Cost functions

Two cost functions, Y_{CoD} and Y_{RDC} , are defined for the estimation of the CoD and RDC, respectively. Under ideal conditions, a non-distorted feature P_{iu} , its corresponding radially distorted position P_{id} and the CoD are collinear; however, a slight error in the CoD position breaks the aforementioned condition and a triangle is formed with the three points. Therefore, we adopt as a cost function Y_{CoD} the sum of the

areas of all the triangles formed by the current CoD_H and the matched P_{pu} and P_{iuH} ; i.e., the areas formed by the aforementioned points in the pattern plane. The triangles' areas are efficiently computed using determinants.

Provided a detected pattern with N corners, the area of the k^{th} triangle defined by the $CoD_H = (C_{Hx}, C_{Hy})$, $P_{pu}^k = (x_{pu}^k, y_{pu}^k)$ and $P_{iuH}^k = (x_{iuH}^k, y_{iuH}^k)$, is given by:

$$A^k = \frac{1}{2} |\det(M^k)| \quad (7)$$

where M^k is given by:

$$M^k = \begin{pmatrix} 1 & 1 & 1 \\ C_{Hx} & x_{pu}^k & x_{iuH}^k \\ C_{Hy} & y_{pu}^k & y_{iuH}^k \end{pmatrix} \quad (8)$$

Finally, the new CoD is estimated by minimizing the following cost function Y_{CoD} :

$$CoD = \min_{(C_x, C_y)} Y_{CoD} = \min_{(C_x, C_y)} \sum_{k=1}^N A^k \quad (9)$$

The RDC cost function Y_{RDC} , is defined as the sum of the Euclidean distances $P_{pu}^k P_{iuH}^k$ between the matches $P_{pu}^k = (x_{pu}^k, y_{pu}^k) \leftrightarrow P_{iuH}^k = (x_{iuH}^k, y_{iuH}^k) \forall k$.

The radial distortion coefficients Λ are thus obtained by minimizing the sum of the aforementioned distances as follows:

$$\Lambda = \min_{\Lambda} Y_{RDC} = \min_{\Lambda} \sum_{k=1}^N \overline{P_{pu}^k P_{iuH}^k} \quad (10)$$

where P_{iuH}^k are computed using (4) and (6). The unconstrained optimization of (9) and (10) was implemented using the Matlab® function fminunc.

We define the parameters' vector for iteration r as $\Delta_r = [C_x, C_y, \lambda_1, \lambda_2, \dots, \lambda_L]$. The iterative optimization of the two cost functions Y_{CoD} and Y_{RDC} is performed and is stopped when the following condition is satisfied:

$$\|\Delta_r - \Delta_{r-1}\|_1 < T \quad (11)$$

where $\|\cdot\|_1$ is the ℓ_1 -norm and T is a threshold whose value was experimentally set to 5×10^{-4} . This value is independent

Table 2. Average radial distortion error of the proposed method for pincushion radial distortion; i.e., $\lambda_{1d} > 0$.

λ_{1d}	$\sigma=0$	$\sigma=0.5$	$\sigma=1$	$\sigma=1.5$	$\sigma=2$	$\sigma=2.5$	$\sigma=3$
0.1	0.001	0.021	0.033	0.006	0.167	0.150	0.167
0.2	0.008	0.005	0.018	0.080	0.143	0.054	0.135
0.3	0.023	0.039	0.024	0.008	0.026	0.060	0.094
0.4	0.050	0.061	0.015	0.081	0.066	0.053	0.015
0.5	0.089	0.124	0.104	0.067	0.083	0.075	0.055
0.6	0.142	0.188	0.193	0.212	0.322	0.046	0.011
0.7	0.209	0.245	0.269	0.233	0.211	0.170	0.193
0.8	0.291	0.377	0.347	0.383	0.259	0.319	0.334
0.9	0.389	0.519	0.464	0.513	0.457	0.531	0.512

of the level of distortion in the test image and of the amount of noise that can be present in the corners' positions.

4. RESULTS

In order to illustrate the performance of the proposed algorithm under noisy estimation of the pattern corners we synthetically distorted a pattern using a second-order polynomial radial distortion model (1) as follows:

$$\begin{aligned} x_d &= (x_u - C_{sx})(1 + \lambda_{1d}r_d^2) + C_{sx} \\ y_d &= (y_u - C_{sy})(1 + \lambda_{1d}r_d^2) + C_{sy} \end{aligned} \quad (12)$$

where r_d is computed as in (3) and (C_{sx}, C_{sy}) represents the CoD position used in the simulations. The polynomial coefficient λ_{1d} was varied from -0.9 to -0.1 with a step-size of 0.1. A zero-mean Gaussian noise $\mathcal{N}(0, \sigma)$ was added to the ground-truth positions of the distorted corners. The noise standard deviation σ was varied from 0 to 3 pixels with a step-size of 0.5 pixels. Monte Carlo simulations with 150 random trials were performed for every value of λ_{1d} and σ .

The radial distortion of a pixel is defined as $|r_d - r_u|$ [7], where r_d and r_u are, respectively, the distorted and undistorted radii, defined as the Euclidean distances from the corresponding distorted or undistorted pixel to the CoD. Fig. 2 shows the plot of the radial distortion versus the distorted radius for a pattern synthetically distorted using (12) with $\lambda_{1d} = -0.5$ and under noiseless conditions ($\sigma = 0$) for the pattern corners (ground-truth solid black curve). Fig. 2 also shows the plots of radial distortion versus the distorted radius that are generated based on the estimated RD parameters using the proposed method (dashed red curve) and the method of [13] (dotted blue curve).

The average radial distortion error defined as the average of the absolute difference between the ground-truth radial distortion curve in Fig. 2 and the estimated one is used as a performance evaluation metric. Comparative results for the method presented in [13] and the proposed one are presented in Table 1 for $-0.9 \leq \lambda_{1d} \leq -0.1$ and for different noise levels. Table 2 presents results of the average radial distortion error for $\lambda_{1d} = 0.1, 0.2, \dots, 0.9$. Results from [13] have not

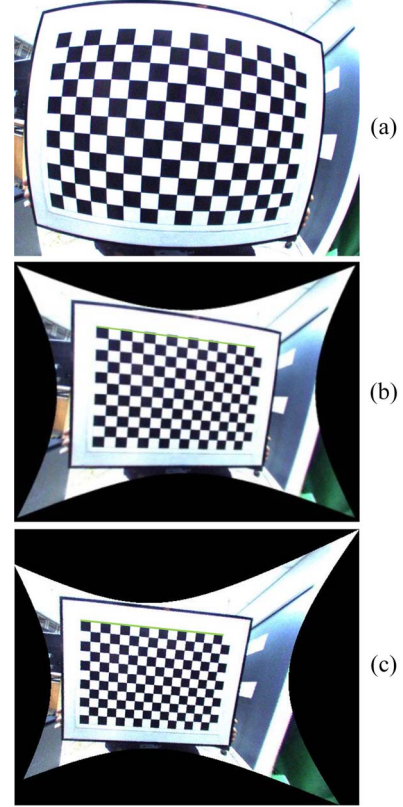


Fig. 3. Radial distortion correction applied to a test image: (a) original distorted image taken from [13], (b) undistorted results using the algorithm of [13], and (c) undistorted result using the proposed method.

been included in this table since [13] fails for distorted images with $\lambda_{1d} > 0$; i.e., images with a pincushion-like radial distortion.

Finally, in order to provide a qualitative comparison we applied the proposed algorithm to the test image used in [13]. The undistorted image using the algorithm of [13] and the proposed one are shown in Figs. 3(b) & 3(c), respectively. From Fig. 3, it can be seen that the proposed method provides a better reconstruction of straight lines in the scene, as compared to the method of [13]. This is especially apparent when comparing the upper borders in Figs. 3(b) & 3(c).

5. CONCLUSION

A noise-robust radial distortion correction method is presented to estimate the radial distortion coefficients as well as the center of distortion through an alternating optimization process. The algorithm was tested for different values of radial distortion parameters as well as under different amounts of noise. Experimental results with synthetic and real distorted images show that the proposed method results in an improved performance in terms of estimation accuracy and also in terms of robustness to noisy conditions.

6. REFERENCES

- [1] Juyang Weng, Paul Cohen, and Marc Herniou, “Camera calibration with distortion models and accuracy evaluation,” *IEEE Trans. on Pattern Analysis and Machine Intelligence*, vol. 14, no. 10, pp. 965–980, 1992.
- [2] Wenjuan Ma and Yuncai Liu, “A curve-fitting method for correcting radial distortion,” in *2nd IEEE International Congress on Signal Processing*, 2009, pp. 1–4.
- [3] Zhengyou Zhang, “A flexible new technique for camera calibration,” *IEEE Trans. on Pattern Analysis and Machine Intelligence*, vol. 22, no. 11, pp. 1330–1334, 2000.
- [4] Anup Basu and Sergio Licardie, “Alternative models for fish-eye lenses,” *Elsevier Pattern Recognition Letters*, vol. 16, no. 4, pp. 433–441, 1995.
- [5] C. Brown Duane, “Close-range camera calibration,” *Photogrammetric Engineering*, vol. 37, pp. 855–866, 1971.
- [6] Andrew W Fitzgibbon, “Simultaneous linear estimation of multiple view geometry and lens distortion,” in *IEEE Conference on Computer Vision and Pattern Recognition*, 2001, vol. 1, pp. I–125.
- [7] Richard Hartley and Sing Bing Kang, “Parameter-free radial distortion correction with center of distortion estimation,” *IEEE Trans. on Pattern Analysis and Machine Intelligence*, vol. 29, no. 8, pp. 1309–1321, 2007.
- [8] Frederic Devernay and Olivier Faugeras, “Straight lines have to be straight,” *Springer-Verlag Machine Vision and Applications*, vol. 13, no. 1, pp. 14–24, 2001.
- [9] Roger Y Tsai, “A versatile camera calibration technique for high-accuracy 3d machine vision metrology using off-the-shelf tv cameras and lenses,” *IEEE Journal of Robotics and Automation*, vol. 3, no. 4, pp. 323–344, 1987.
- [10] Thorsten Thormählen, Hellward Broszio, and Ingolf Wassermann, “Robust line-based calibration of lens distortion from a single view,” in *Proceedings of MIRAGE INRIA*, 2003, pp. 105–112.
- [11] Simone Graf and Tobias Hanning, “Analytically solving radial distortion parameters,” in *IEEE Conference on Computer Vision and Pattern Recognition*, 2005, vol. 2, pp. 1104–1109.
- [12] Reimar K Lenz and Roger Y Tsai, “Techniques for calibration of the scale factor and image center for high accuracy 3-d machine vision metrology,” *IEEE Trans. on Pattern Analysis and Machine Intelligence*, vol. 10, no. 5, pp. 713–720, 1988.
- [13] Xianghua Ying, Xiang Mei, Sen Yang, Ganwen Wang, and Hongbin Zha, “Radial distortion correction from a single image of a planar calibration pattern using convex optimization,” in *IEEE International Conference on Image Processing*, 2014, pp. 3440–3443.
- [14] Janne Heikkilä, “Geometric camera calibration using circular control points,” *IEEE Trans. on Pattern Analysis and Machine Intelligence*, vol. 22, no. 10, pp. 1066–1077, 2000.
- [15] Gideon P Stein, “Lens distortion calibration using point correspondences,” in *IEEE Conference on Computer Vision and Pattern Recognition*, 1997, pp. 602–608.
- [16] David Claus and Andrew W Fitzgibbon, “A rational function lens distortion model for general cameras,” in *IEEE Conference on Computer Vision and Pattern Recognition*, 2005, vol. 1, pp. 213–219.
- [17] Jean-Philippe Tardif, Peter Sturm, and Sébastien Roy, “Self-calibration of a general radially symmetric distortion model,” in *9th European Conference on Computer Vision*, pp. 186–199, 2006.
- [18] R Matt Steele and Christopher Jaynes, “Overconstrained linear estimation of radial distortion and multi-view geometry,” in *European Conference on Computer Vision*, pp. 253–264. Springer, 2006.
- [19] Car O. Geiger A., Moosmann F. and Schuster B., “Automatic camera and range sensor calibration using a single shot,” in *IEEE International Conference on Robotics and Automation*, 2012, pp. 3936–3943.
- [20] Aiqi Wang, Tianshuang Qiu, and Longtan Shao, “A simple method of radial distortion correction with centre of distortion estimation,” *Journal of Mathematical Imaging and Vision*, vol. 35, no. 3, pp. 165–172, 2009.
- [21] Luis Alvarez, Luis Gómez, and J Rafael Sendra, “An algebraic approach to lens distortion by line rectification,” *Journal of Mathematical Imaging and Vision*, vol. 35, no. 1, pp. 36–50, 2009.
- [22] Rahul Swaminathan and Shree K Nayar, “Nonmetric calibration of wide-angle lenses and polycameras,” *IEEE Trans. on Pattern Analysis and Machine Intelligence*, vol. 22, no. 10, pp. 1172–1178, 2000.
- [23] Moumen Taha El-Melegy, Aly Farag, et al., “Statistically robust approach to lens distortion calibration with model selection,” in *IEEE Conference on Computer Vision and Pattern Recognition*, 2003, vol. 8, pp. 91–91.
- [24] R. I. Hartley and A. Zisserman, *Multiple View Geometry in Computer Vision*, Cambridge University Press, ISBN: 0521540518, second edition, 2004.